The integrity of a cholesterol-binding pocket in Niemann–Pick C2 protein is necessary to control lysosome cholesterol levels

Dennis C. Ko*, Jonathan Binkley†, Arend Sidow†‡, and Matthew P. Scott*‡§¶

Departments of *Developmental Biology, ‡Genetics and †Pathology, §Howard Hughes Medical Institute, Beckman Center B300, 279 Campus Drive, Stanford University School of Medicine, Stanford, CA 94305-5329

This contribution is part of the special series of Inaugural Articles by members of the National Academy of Sciences elected on April 27, 1999.

Contributed by Matthew P. Scott, January 3, 2003

The neurodegenerative disease Niemann–Pick Type C2 (NPC2) results from mutations in the *NPC2* (*HE1*) gene that cause abnormally high cholesterol accumulation in cells. We find that purified NPC2, a secreted soluble protein, binds cholesterol specifically with a much higher affinity (K_d = 30–50 nM) than previously reported. Genetic and biochemical studies identified single amino acid changes that prevent both cholesterol binding and the restoration of normal cholesterol levels in mutant cells. The amino acids that affect cholesterol binding surround a hydrophobic pocket in the NPC2 protein structure, identifying a candidate sterol-binding location. On the basis of evolutionary analysis and mutagenesis, three other regions of the NPC2 protein emerged as important, including one required for efficient secretion.

point mutants | secretion | protein evolution

Niemann–Pick Type C (NPC) is an autosomal-recessive disorder characterized by progressive ataxia, dystonia, and dementia (1). Substantial cell death, particularly in the cerebellum, accounts for some of the symptoms. At the cellular level, mutant cells accumulate cholesterol and other lipids in aberrant compartments with features of late endosomes and lysosomes, and the normal homeostatic response to this excess cholesterol is abolished (2–4).

Our understanding of the molecular basis of this disease has progressed substantially over the last several years, because the two genes damaged by NPC mutations, *NPC1* and *NPC2*, have been identified (5–7). *NPC1* encodes a multiple-membrane-spanning protein containing sequences similar to the sterol cleavage activating protein (SCAP) regulator of cholesterol metabolism and the receptor Patched, a transducer of the Hedgehog family of protein signals. Mutations in *NPC1* are responsible for ≈95% of the NPC cases (8). The exact role that NPC1 plays in maintaining normal levels of cholesterol in late endosomes and lysosomes remains mysterious. Even less is known about the NPC2 [human epididymis (HE1)] protein, the loss of which is responsible for 5% of NPC cases.

NPC2 is a small secreted glycoprotein originally identified as a transcript enriched in the HE1 (9). The porcine HE1 homolog was reported to bind cholesterol with micromolar affinity (K_d = 2.3 μM; ref. 10), information that was crucial in identifying HE1 as a candidate *npc2* gene product (7). However, the similarity between the reported K_d and the solubility of cholesterol in aqueous solution (5 μM, Merck Index) warrants reexamination of the strength and specificity of this interaction. If the binding is meaningful, NPC2 activity could be altered when cholesterol is bound, thus serving as a sensor of cholesterol levels, accessibility, or location. Alternatively, NPC2 could process or transport cholesterol. Resolving these questions is crucial for determining why cholesterol accumulates in people lacking functional NPC2 protein and for designing rational treatment strategies.

In this report, we combine *in vitro* binding experiments, genetic analysis, a quantitative cell-based assay of NPC2 function, and sequence evolution information to investigate how NPC2 works. In the accompanying paper by Friedland *et al.* (11), the crystal structure of NPC2 is reported, further revealing the unique properties of the proposed cholesterol-binding site.

Materials and Methods

Plasmids. Full-length mouse NPC2 cDNA was amplified from Clone 408396 (Research Genetics, Huntsville, AL). The PCR product was cloned into the *Eco*RI and *Xho*I sites in pcDNA3 (Invitrogen) to yield pNPC2. For the myc 6xHis-tagged construct, the PCR product was inserted into the *Eco*RI and *Kpn*I sites in pcDNA 3.1(−)/myc-his A (Invitrogen) to yield pNPC2myc-his. In both cases, the insert was fully sequenced. To generate stably expressing cells, a bicistronic construct was made by inserting the 5.2-kb *Xba*I/*Afl*II fragment from pNPC2myc-his into pIRESpuro2 (CLONTECH) digested with *Nhe*I and *Afl*II to yield pNPC2myc-his-puro. Point mutants were generated by using QuikChange (Stratagene) according to the manufacturer's instructions.

Cell Culture and Establishment of Chinese Hamster Ovary (CHO)-KI Cells Stably Expressing NPC2-myc-his. CHO-KI cells (American Type Culture Collection) were grown in F12 (10% FBS/10 μg/ml gentamicin). Human NPC2 fibroblasts were the kind gift of Dan Ory (Washington University, St. Louis) and were grown in DMEM (10% FBS/1 mM sodium pyruvate/0.1 mM nonessential amino acids/2 mM glutamine/penicillin/streptomycin). For experiments involving lipid-free media, cells were washed three times and then incubated in DMEM (1% BSA/0.1 mM nonessential amino acids/2 mM glutamine/penicillin/streptomycin).

For the generation of stably expressing NPC2-myc-his cells, CHO-KI cells were transfected with pNPC2myc-his-puro by using Fugene6 (Roche Molecular Biochemicals). Forty-eight hours posttransfection, the cells were passaged, and transformants were selected with 12 μg/ml puromycin. After 2 weeks of selection, colonies were picked with cloning rings. The conditioned medium from each isolated colony was screened for NPC2-myc-his production level by protein blotting with the anti-myc 9E10 antibody (Sigma). For detection of intracellular NPC2-myc-his, a polyclonal NPC2 antibody (a gift from Peter Lobel, Robert Wood Johnson Medical School, Piscataway, NJ) was used to avoid problems due to degradation of the myc-his tag.

Purification of NPC2. To purify NPC2-myc-his, stably expressing cells were split on day 0 into 10-cm dishes. The next day, cells were washed, and the medium was changed to CD CHO

Abbreviations: NPC, Niemann–Pick Type C; ECR, evolutionarily constrained regions.

¶To whom correspondence should be addressed. E-mail: scott@cmgm.stanford.edu.

 www.pnas.org/cgi/doi/10.1073/pnas.0530027100

serum-free media (Invitrogen). On day 4, the medium was harvested and put through a 0.2-μm syringe filter. Conditioned medium was concentrated by using Centriprep YM10 concentrators (Millipore) and bound to 0.1 g of Ni-TED resin (Active Motif, Carlsbad, CA) for 30 min at room temperature. The resin was washed twice with 10 ml of wash buffer (50 mM sodium phosphate/150 mM NaCl, pH 7.0). Elution of NPC2-myc-his was carried out in 1 ml of elution buffer (wash buffer + 150 mM imidazole). The eluate was concentrated and separated from imidazole by using four successive rounds of centrifugation with a Centricon YM10 (Millipore). Purification of mutant proteins was carried out similarly, except transiently transfected cells were used.

For further purification, gel filtration was carried out by using an Akta FPLC and Superdex 75 HR 10/30 column (Pharmacia). The column was equilibrated in PBS with 0.01% Triton X-100 to prevent sticking of NPC2. NPC2 protein eluted in fractions between the 17- and 44-kDa molecular mass markers as expected. Acetone precipitation was carried out to delipidate NPC2. Acetone was added to 80% of final volume. The protein solution was incubated on dry ice for 3 h, centrifuged, washed twice with 100% acetone, and dried under vacuum. Complete removal of cholesterol was verified by using [^{3}H]cholesterol.

NPC2 Radioligand-Binding Assay. The cholesterol-binding assay was modified from ref. 10. Purified NPC2 protein was incubated with [^{3}H]cholesterol (Perkin–Elmer Life Sciences) for 30 min at 30°C in PBS (10 mM sodium phosphate/130 mM NaCl) at the indicated pH. Free and bound cholesterols were separated by centrifugation (750 $\times$ *g*, 2 min) through a CentriSep gel filtration column (Princeton Separations, Adelphia, NJ) preequilibrated in the buffer used for binding along with 0.01% Triton X-100 to reduce binding of NPC2 to the column. Due to variability between batches of CentriSep columns, each lot was tested to ensure that free cholesterol was efficiently retained, and that a significant portion of NPC2 protein passed through the column. The B_{max} values obtained in saturation experiments varied and were always less than the value predicted by the amount of protein because of column-to-column variability in the amount of NPC2 protein that adsorbed nonspecifically. For this reason, the same column was used to separate bound and free cholesterol for each point in a saturation curve, after determining that essentially no counts carried over. Radioactivity was measured with a Beckman LS5000 CE Scintillation Counter (Beckman Coulter). Cholesterol, oleic acid, and cholesteryl oleate used in competition experiments were from Sigma. Curve fitting and estimation of K_d and rate constants were done with PRISM (GraphPad, San Diego).

Filipin Staining Assay. Filipin staining was carried out as described (12). To quantitatively compare activity of NPC2 proteins, amounts of NPC2 proteins were measured by protein blotting, scanned, and fit to a standard curve of wild-type NPC2 protein. Conditioned medium or purified NPC2 protein was applied to NPC2 fibroblasts grown in eight-well chamber slides (Lab-Tek). After 3 days, cells were filipin stained and imaged with an epifluorescence microscope (Zeiss) and charge-coupled device camera (Princeton Instruments, Trenton, NJ). Punctate filipin fluorescence was measured by thresholding and quantifying by using METAMORPH (Universal Imaging, Media, PA). Fitting to a dose–response curve to determine EC_{50} values was done with PRISM.

Computational Methods. Local evolutionary rates over the primary sequence of NPC2 protein were estimated by using the Evolution Structure Function method (13). Briefly, a multiple sequence alignment of vertebrate NPC2 homologs was made with CLUSTALW (14), a phylogenetic tree was built by using the program SEMPHY (15) and, holding the branching pattern of this tree constant, SEMPHY was used to calculate the number of substitutions per site in each window of 11 amino acid residues over the entire alignment. The reported rate values were derived by first dividing the number of substitutions per site in each window by the average of all windows (yielding the "relative rate") and then smoothing the relative rates using a 10-position-wide moving window arithmetic average.

The 3D-PSSM web-based homology server (16, 17) identified the Der p 2 dust mite allergen as an excellent template for modeling the NPC2 protein structure (*E* value 7.14e-13) based on multiple sequence alignment, secondary structure prediction, and solvation potential. The Der p 2 structure is a β sandwich, and all six cysteine residues involved in disulfides are conserved between the two proteins. Four gaps are present in the alignment, but these are all in loop regions and are unlikely to affect the overall structure of the protein. Higher similarity scores could be obtained by shifting two single amino acid gaps by two amino acids (from D26 to P24 and from K75 to G77). This alignment was submitted to SWISS-MODEL (18) to obtain the homology model of NPC2 used to guide the generation of point mutants. The creation of images of the NPC2 homology model and crystal structure, as well as identification of cavities, was done by using the SWISS-PDB VIEWER (18).

Results

Purification of Functional Tagged NPC2 Protein and Stoichiometry of NPC2 Action. The novelty of the NPC2 protein and the lack of any known mechanism of its action prompted a genetic structure–function study of its properties. To this end, we purified wild-type and mutant NPC2 proteins, starting from a culture medium into which cells had released NPC2. Previous studies of NPC2 used NPC2-conditioned media (7) or NPC2 purified from porcine epididymal fluid (10). These procedures are not practical for studying a substantial number of mutant proteins, so we developed a rapid affinity-purification procedure.

To facilitate purification, we fused myc and 6xHIS tags to the C terminus of mouse NPC2. The addition of the tags has no effect on the function of the protein, as judged by the ability of conditioned media to genetically complement fibroblasts from a homozygous *npc2* patient (Fig. 1*A*). Comparable amounts of NPC2- or NPC2-myc-his-conditioned media restored normal cholesterol levels, based on staining with the fluorescent antibiotic filipin.

NPC2-myc-his protein was purified from conditioned media from stably transfected CHO-KI cells, as described in *Materials and Methods*. The purity, assessed by staining for total protein, was estimated at $\approx$60% after the Ni-affinity step and >90% after gel filtration (Fig. 1*B*). Complementation of *npc2* cells showed that the purified protein was highly active, with an EC_{50} of 1.5 nM (assuming an average molecular mass of 27 kDa) (Fig. 1*C*). Depending on the passage number of the cells and how quickly the cells were proliferating, this value varied by roughly 5-fold in either direction. The results of the purification are summarized in Fig. 1*D*.

The abundance of NPC2 protein in rescued cells informs ideas about possible roles of NPC2 as a cholesterol carrier or sensor. We estimated the amount of NPC2 that had entered rescued cells by using protein blots of cell extracts after incubation with different amounts of tagged NPC2 protein (Fig. 1*E*). A steady-state level of $\approx 4.5 \times 10^5$ molecules of NPC2 is required to fully rescue an *npc2* fibroblast. Incubating cells with excess NPC2 protein increases the amount of internalized NPC2 detected but does not further reduce lysosomal cholesterol levels.

The $\approx 4.5 \times 10^5$ molecules of NPC2 may be contrasted with the 2.5×10^9 cholesterol molecules per cell, of which $\approx$6% is in lysosomes (19, 20). In a cell lacking functional NPC1 or NPC2, the amount of cholesterol in lysosomes increases drastically (up

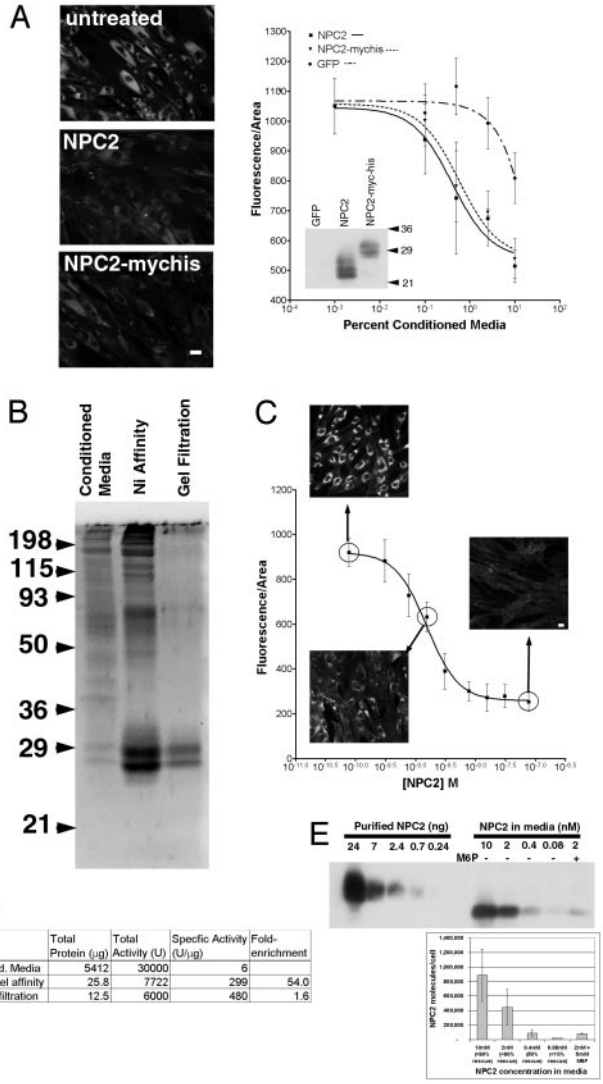

	Total Protein (μg)	Total Activity (U)	Specfic Activity (U/μg)	Fold-enrichment
Cond. Media	5412	30000	6	
Nickel affinity	25.8	7722	299	54.0
Gel filtration	12.5	6000	480	1.6

Fig. 1. Purified tagged NPC2 protein complements cholesterol accumulation in *npc2* cells with ≈4.5 × 10^5 molecules of protein/cell at steady-state being sufficient for rescue. (*A*) NPC2 with C-terminal myc and 6xHis tags is as effective as wild-type NPC2 in rescuing *npc2* fibroblasts. After treatment for 3 days with 10% conditioned media from CHO-KI cells transiently transfected with NPC2 or NPC2-myc-his, *npc2* fibroblasts were stained with filipin. (Bar = 20 μm.) Dose–response curves quantifying the average filipin fluorescence/area show that NPC2 and NPC2-myc-his are similarly effective in clearing cholesterol accumulation in *npc2* fibroblasts (EC_{50} ≈ 0.5%). Much less activity is found in the enhanced GFP conditioned media (EC_{50} ≈ 10%) due to the endogenous NPC2 produced by CHO cells. Error bars are standard deviations of fluorescence/area from seven imaged fields. (*Inset*) Protein blot of conditioned media probed with anti-NPC2. NPC2 and NPC2-myc-his are expressed at similar levels. (*B*) Assessment of NPC2-myc-his purification. NPC2-myc-his conditioned media and purified fractions after nickel-affinity purification and gel filtration were resolved by SDS/PAGE in a 12% gel and stained for total protein with SYPRO Ruby. NPC2-myc-his purified from conditioned media from stably expressing cells migrates as a doublet with an apparent molecular mass of 27–29 kDa. (*C*) The EC_{50} of purified NPC2 in complementing *npc2* cells is 1.5 nM. Addition of NPC2-myc-his purified by the two-step protocol to *npc2* fibroblasts induces a dose-dependent decrease in lysosomal cholesterol, as assessed by filipin staining. Error bars are standard deviations of fluorescence/area from seven imaged fields. (*D*) Purification table of NPC2-myc-his two-step purification. Total protein at each step was determined by Bradford assay, and activity was determined by filipin staining with the amount necessary for 50% rescue defined as 1 unit. (*E*) The number of NPC2 molecules required in a single *npc2* cell for rescue is ≈4.5 × 10^5. *npc2* cells were incubated overnight with the indicated amount of purified NPC2-myc-his. Longer incubation (3 days) did not alter the amount of NPC2-myc-his detected. Incubation of conditioned media along with 5 mM mannose-6-phosphate to block uptake of the NPC2 protein was done concurrently to ensure that the protein detected was specific. Cell extracts along with known amounts of purified NPC2-myc-his protein were immunoblotted with anti-NPC2. A single band of ≈22 kDa was detected. The amount of NPC2 protein within each cell was estimated based on standard curves of purified NPC2-myc-his and dividing by the total number of cells loaded into the lane (2 × 10^5). The graph shows the mean and standard deviations from three experiments. Cells incubated with the indicated concentration of protein for 3 days were filipin stained concurrently to determine the degree of rescue.

to 10-fold in *npc1* fibroblasts; ref. 20). Dividing the number of excess lysosomal cholesterol molecules (1.35 × 10^9) by the number of NPC2 molecules required for rescue (≈4.5 × 10^5) suggests that each NPC2 molecule causes the redistribution of ≈3,000 cholesterol molecules or more if only some NPC2 molecules are active. Because full rescue requires 2–3 days, the rate of mobilization is ≈1 cholesterol/NPC2/minute. Thus, for rescue to occur, a small amount of NPC2 protein must stimulate the movement of a substantially greater number of cholesterol molecules to the endoplasmic reticulum for esterification and/or to the plasma membrane for transfer to extracellular acceptors.

NPC2 Binds Cholesterol Specifically with Nanomolar Affinity. From three independent sets of measurements, we determined that NPC2 binds to cholesterol with a much greater affinity than previously reported (10). Measurements of association and dissociation were made to assess the kinetics of the interaction and to determine proper conditions for conducting binding experiments. For measuring association rate, purified NPC2-myc-his was incubated with [^{3}H]cholesterol for various periods at 30°C followed by gel filtration centrifugation. Nearly maximum binding was achieved in 5 min (k_{obs} = 0.37 min^{-1}) (Fig. 2*A*). The dissociation of cholesterol from NPC2 was measured by allowing NPC2-myc-his and [^{3}H]cholesterol to bind to equilibrium and then adding a 50-fold excess of cold cholesterol. The off-rate for the reaction was calculated as 0.18 min^{-1}, which corresponds to a half-life of 4 min. The off-rate was combined with the observed association constant and the initial cholesterol concentration to determine the true on-rate {k_{on} = (k_{obs} − k_{off})/[radioligand] = 5.8 × 10^6 M^{-1}·min^{-1}}. Calculation of the K_d as k_{off}/k_{on} gives a value of 30 nM.

A similar K_d value was obtained with saturation binding experiments (Fig. 2*B*). This measurement is complicated by increased flow-through in the gel filtration column at concentrations >≈300 nM (not shown). Regardless, binding of NPC2 to cholesterol begins to saturate below this concentration, and analysis of the saturation curves from eight sets of measurements gives a K_d (K_d = 27 ± 15 nM), in agreement with the value obtained from kinetic measurements.

NPC2 comigrates with lysosome markers on sucrose gradients (7). For this reason, we determined whether cholesterol is bound at the acidic lysosomal pH of 5.0. The saturation curve obtained at pH 5.0 in phosphate buffer was similar to that obtained under neutral conditions, giving a K_d of 32 ± 24 nM (Fig. 2*B*).

Experiments in which cholesterol competed with other hydrophobic molecules for binding to NPC2 gave a binding constant in agreement with the kinetic and saturation binding experiments (EC_{50} = 60 nM; by the Cheng–Prussof equation for homologous competition, K_d = EC_{50} − [chol] = 50 nM; Fig. 2*C*). Tests were done with oleic acid and cholesteryl oleate, molecules chosen for their hydrophobicity and similarity to cholesterol and because NPC1 can transport fatty acids in bacteria (21). Neither oleic acid nor cholesteryl oleate competes with [^{3}H]cholesterol for NPC2 binding, even when added at 8 μM (an 800-fold excess) (Fig. 2*C*). We conclude that NPC2 specifically binds to cholesterol and not to other lipids that are found in lysosomes.

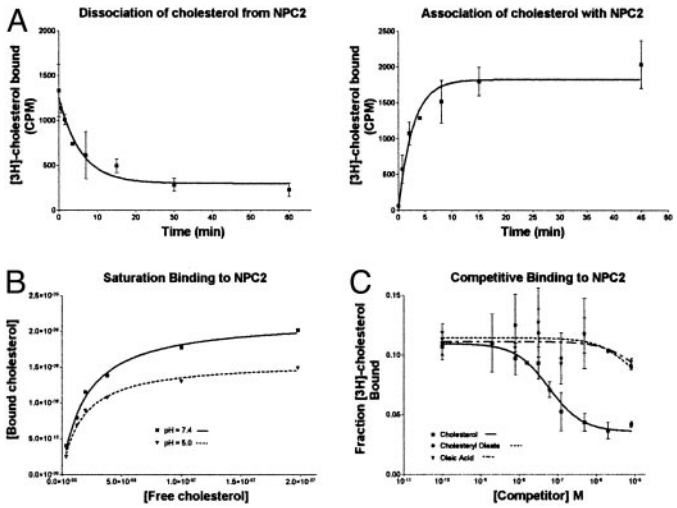

Fig. 2. Purified NPC2 protein binds cholesterol with a K_d of ≈30–50 nM. (*A*) Association and dissociation of cholesterol to NPC2-myc-his. Purified NPC2-myc-his (0.8 μg/ml) was incubated with 10 nM [^{3}H]cholesterol in PBS (pH = 7.4) at 30°C. For the association curve, aliquots were removed at the times indicated and immediately centrifuged through a centrisep column to separate free and bound cholesterol, and bound counts were measured. For the dissociation curve, 500 nM cold cholesterol was added at time 0 to block free sites. At the times indicated, aliquots were taken and analyzed as above. Nonlinear regression analysis of the curves reveals k_{off} = 0.18 min^{-1}, $k_{on} = 5.8 \times 10^6$ M^{-1}·min^{-1}, and $K_d = k_{off}/k_{on}$ = 30 nM. Error bars show the standard deviations of triplicate measurements. (*B*) Saturation binding of cholesterol to NPC2-myc-his. Purified NPC2-myc-his (0.5 μg/ml) was incubated with the indicated amount of [^{3}H]cholesterol in PBS at pH 7.4 or 5.0 for 30 min at 30°C. Bound counts were collected by gel filtration and measured. Analysis of the saturation curves shown gives K_d = 20 nM for pH = 7.4 and K_d = 17 nM for pH = 5.0. From at least four similar measurements, we obtained K_d values of 27 ± 15 nM at pH = 7.4 and 32 ± 24 nM at pH = 5.0. (*C*) Cholesteryl oleate and oleic acid are unable to compete for the NPC2-myc-his cholesterol binding site. Purified NPC2-myc-his (0.5 μg/ml) was incubated with 10 nM [^{3}H]cholesterol and the indicated amount of cold competitor for 30 min at 30°C. Bound counts were collected by gel filtration and measured. Cholesterol is able to compete for binding with a calculated K_d of 50 nM, whereas oleic acid and cholesteryl oleate show no competition even at the highest concentration tested (8 μM). Error bars show the standard deviations of measurements taken from three independent experiments.

Rationale for Site-Directed Mutagenesis: Evolutionary Analysis and Homology Modeling. The relevance of the NPC2-cholesterol interaction *in vivo* was addressed by determining whether mutated forms of NPC2 that are unable to bind cholesterol can restore normal cholesterol levels in *npc2* fibroblasts. The cholesterol-binding activity of NPC2 could be essential for regulating cholesterol levels in cells, a nonessential activity, or an artifact of *in vitro* analysis. A tight correlation between mutations that block cholesterol binding and those that block restoration of normal cholesterol levels in cells would support the importance of cholesterol binding. Conversely, NPC2 protein variants able to rescue the cell phenotype but unable to bind cholesterol would argue against the importance of the binding.

To aid in designing mutants that disrupt NPC2 function, we identified evolutionarily constrained regions (ECRs) of the protein (13) and developed a homology model of the NPC2 protein structure. The ECR procedure assigns sequence conservation scores by comparing sliding windows of 11 aa. Analysis using all available vertebrate proteins related to NPC2 (human, mouse, pig, dog, cow, and zebrafish proteins) identified four regions with strong conservation (ECRs A, B, C, and D; Fig. 3). A second tool that aided the design of mutants is a homology model of NPC2 based on the Der p 2 dust-mite allergen, a protein with 23% identity and 63% similarity over the entire protein.

Single amino acids were chosen on the basis of evolutionary conservation and the homology model as candidate residues that might be involved in cholesterol binding. Cholesterol-binding sites in other proteins have been modeled to consist of a hydrophobic binding site and a hydrogen bond between the hydroxyl group of cholesterol and a nearby basic residue (22, 23). We made amino acid changes that are predicted to interfere with both these classes of noncovalent interaction. To interfere with possible hydrophobic interactions, we mutated several small solvent-exposed hydrophobic residues to phenylalanine (I15F, L54F, V64F, and V96F), reasoning that they might block sterol binding through steric hindrance. Several aromatic residues (F66A, Y90A, Y100A, W109A, and W122A) were changed to alanine to disrupt stacking with the cholesterol ring structure. To interfere with hydrogen bonding to the cholesterol hydroxyl group, each of the conserved charged residues was changed to alanine (D7A, K32A, H56A, D72A, K75A, K97A, E99A, K104A, E108A, and D114A). Three other amino acids that are completely conserved among vertebrates were mutated to alanine: S35A is located at the minima of one of the ECRs, N39A

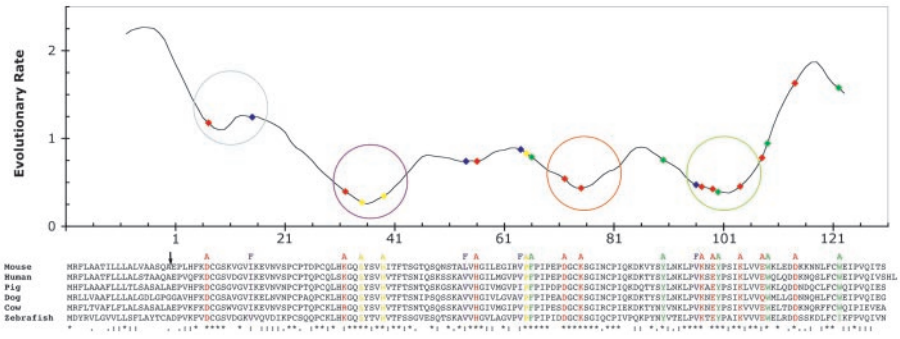

Fig. 3. Evolutionary analysis of the NPC2 protein reveals amino acids predicted to be important for function. A plot of local evolutionary rates across the NPC2 protein is shown, along with the multiple sequence alignment of vertebrate NPC2 homologs used to estimate those rates and the mutations constructed within the NPC2 protein. The values plotted along the *y* axis are derived from the average number of amino acid substitutions per site (*Materials and Methods*) for residues at the corresponding *x* axis position. The circles on the plot mark the four evolutionarily constrained regions (ECRs A, B, C, and D from left to right). The sequence is numbered beginning with the first amino acid after the signal sequence cleavage site (marked by an arrow). Asterisks, colons, or dots below the sequence alignment indicate identical, highly similar, and similar residues, respectively. Mutations made in the mouse sequence are shown as colored amino acid residues; the substituting residue is shown above the mouse sequence. Red indicates conserved charged residues; blue indicates conserved hydrophobic residues predicted to be at least partially surface-exposed; green indicates conserved aromatic residues; and yellow indicates other conserved residues (see text). The positions of the mutations are highlighted on the rate plot with diamonds of the same colors.

is a predicted N-linked glycosylation site, and P65 is in a well-conserved proline-rich stretch of the protein.

Mutations That Disrupt Cholesterol Binding Interfere with Restoration of Normal Cholesterol Levels in *npc2* Fibroblasts. Of the 22 amino acid substitution mutants, three interfered with the cholesterol-binding activity of NPC2. We first eliminated proteins from our analysis that were either poorly translated or poorly secreted. Y90A and W109A accumulated only to very low levels, based on protein blots of lysates from transiently transfected cells. Two mutated NPC2 forms (D7A and I15F) accumulate to normal levels but are very poorly secreted from transfected cells. N39A is also poorly secreted and accumulates as a lower-molecular-weight band in transfected cells, as would be expected if the mutation interferes with glycosylation (not shown).

The 17 proteins that accumulate and are secreted at levels comparable to the wild-type protein were tested for their ability to rescue *npc2* fibroblasts. The medium from cells producing wild-type or mutant protein was applied to *npc2* cells, and the dispersal of filipin-stained cholesterol was monitored. Using a concentration of NPC2 protein that resulted in ≈75% rescue with wild-type protein, we measured the level of rescue achieved with mutant NPC2. Normalized for the amount of NPC2, based on protein blots, K32A, F66A, D72A, K75A, V96F, and Y100A rescued to <70% of the extent of wild type (Fig. 4*A*). Due to the low level of wild-type NPC2 that is secreted from the producing cell line, this assay identifies only mutations that severely affect NPC2 activity.

To more accurately measure activities of the six most severely affected mutant proteins and to assess their cholesterol-binding activities, we purified them with a single nickel-affinity step (Fig. 4*B*). The reduced activity of these mutants is unlikely to be due to misfolding, because all six were produced, glycosylated, and secreted much like the wild-type protein. Quantitative assessment of the mutant protein activities, measuring their rescue of *npc2* fibroblasts at multiple concentrations, showed that all six have severely reduced activity (Fig. 4*C*). The relative amounts of activity of the six purified mutant proteins correlated well with the activity measured in conditioned media. F66A, V96F, and Y100A were most severely affected in both cases. With the removal of endogenous NPC2 and the measurement of a dose–response curve, it became apparent that F66A, V96F, and Y100A have <10% of the wild-type specific activity.

The six loss-of-function mutants were tested for their ability to bind cholesterol in saturation binding experiments. F66A, V96F, and Y100A had no detectable cholesterol binding (Fig. 4*D*). The K_d values for these mutants cannot be quantitatively assessed with this assay, because high nonspecific binding and the poor solubility of cholesterol prevent the use of concentrations >300 nM. Furthermore, any mutation that reduced the half-life of the binding interaction to <30 sec would be expected to give a curve indistinguishable from no binding because of the time required to separate bound from free cholesterol.

F66A, V96F, and Y100A gave curves essentially identical to the no-protein control, indicating a severe decrease in their ability to bind cholesterol. In contrast, the other three mutants with drastically reduced rescuing activity gave cholesterol-binding constants similar to wild type. Mutations that disrupt cholesterol binding but allow stable accumulation and export of the protein have a severely reduced ability to rescue *npc2* cells, suggesting that the cholesterol-binding activity of NPC2 is essential for the control of cellular cholesterol levels.

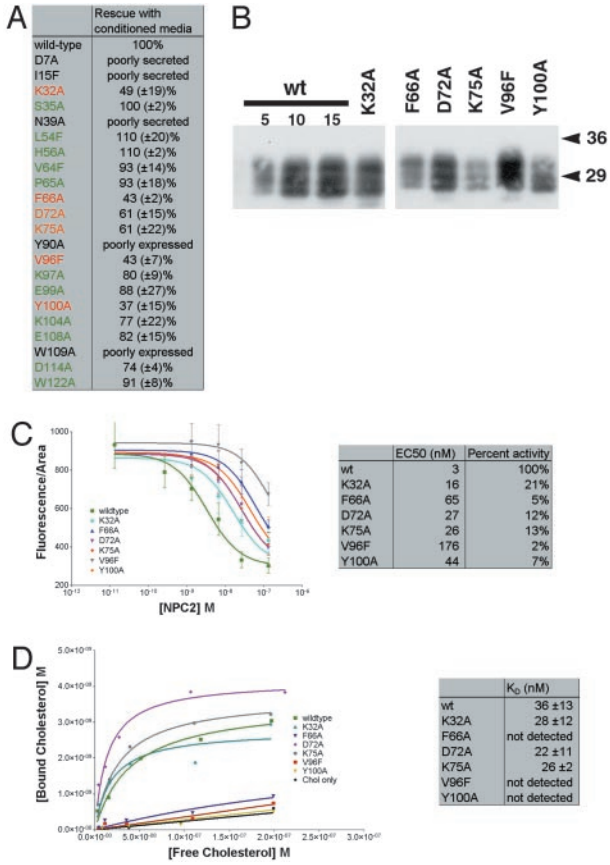

	Rescue with conditioned media
wild-type	100%
D7A	poorly secreted
I15F	poorly secreted
K32A	49 (±19)%
S35A	100 (±2)%
N39A	poorly secreted
L54F	110 (±20)%
H56A	110 (±2)%
V64F	93 (±14)%
P65A	93 (±18)%
F66A	43 (±2)%
D72A	61 (±15)%
K75A	61 (±22)%
Y90A	poorly expressed
V96F	43 (±7)%
K97A	80 (±9)%
E99A	88 (±27)%
Y100A	37 (±15)%
K104A	77 (±22)%
E108A	82 (±15)%
W109A	poorly expressed
D114A	74 (±4)%
W122A	91 (±8)%

	EC50 (nM)	Percent activity
wt	3	100%
K32A	16	21%
F66A	65	5%
D72A	27	12%
K75A	26	13%
V96F	176	2%
Y100A	44	7%

	K_D (nM)
wt	36 ±13
K32A	28 ±12
F66A	not detected
D72A	22 ±11
K75A	26 ±2
V96F	not detected
Y100A	not detected

Fig. 4. Mutations in NPC2 that specifically decrease cholesterol binding interfere with mobilization of lysosomal cholesterol. (*A*) Rescue of *npc2* fibroblasts with NPC2-myc-his conditioned media. A single concentration of wild-type NPC2-myc-his conditioned media was chosen that results in an intermediate level of rescue (≈75%) when added to *npc2* cells. Equivalent amounts of each of the mutants were added to *npc2* cells and analyzed by filipin staining after incubation for 3 days. The level of rescue normalized to 100% for wild type is given as a mean percentage with the standard deviation from at least three independent experiments. Of the 17 mutants assayed, only six showed a significantly reduced level of rescue, and these are labeled in orange (<70% rescue) and red (<50% rescue). (*B*) Protein blot of the six loss-of-function mutants purified from conditioned media. Conditioned media from transiently transfected CHO-KI cells were concentrated and purified by nickel affinity. Protein blotting with anti-myc shows that NPC2-myc-his from transient transfection is secreted as three major bands between 27 and 32 kDa. All three forms are present in each of the mutants. Variation in the amount of protein was corrected for subsequent experiments by comparison with a wild-type standard curve (5–15 μl). (*C*) Dose–response curves for rescue of *npc2* fibroblasts with purified NPC2 proteins. Each of the purified NPC2-myc-his proteins was added at the indicated concentration to *npc2* cells for 3 days, fixed, and filipin stained, and the fluorescence from seven fields was quantified. The EC_{50} value for each is given, along with the activity with wild type normalized to 100%. All six mutants identified by the conditioned media assay have severely reduced activity, with the three most severe mutations (F66A, V96F, and Y100A) exhibiting <10% of wild-type activity. (*D*) Assessment of the cholesterol-binding ability of mutant NPC2 proteins. Each of the purified NPC2-myc-his proteins was incubated with increasing amounts of [^{3}H]cholesterol to measure saturation binding. Calculation of the K_d values from these curves shows that three of the mutants (K32A, D72A, and K75A) bind similarly to wild type, whereas the other three mutants (F66A, V96F, and Y100A) show no detectable binding.

NPC2 Is Not a Sensor of Extracellular Cholesterol. The analyses of mutant proteins show that specific high-affinity binding of cholesterol to NPC2 is likely to be required for maintaining normal cholesterol levels in lysosomes. What purpose could cholesterol binding serve? An unknown NPC2 activity could be regulated by cholesterol binding, within or outside of the cell or both. If NPC2 binds cholesterol outside the cell, it could serve as a sensor of extracellular cholesterol concentration, but this seems unlikely. First, NPC2 protein that is completely delipidated by acetone precipitation is able to rescue *npc2* cells

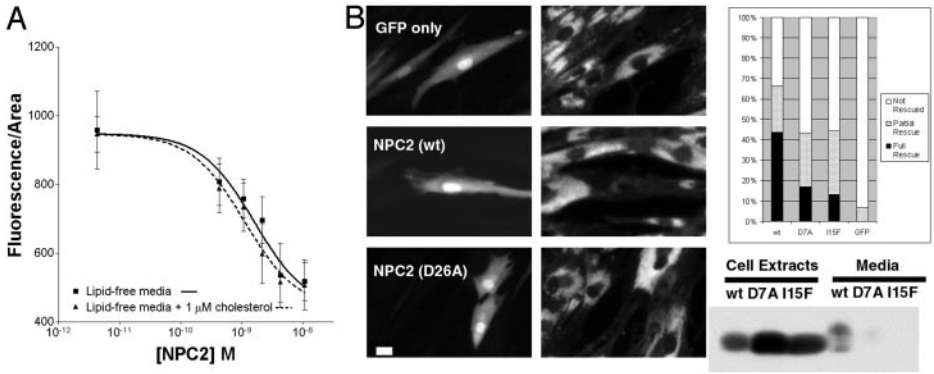

Fig. 5. NPC2 does not function as an extracellular sensor of cholesterol. (*A*) Modulation of extracellular levels of cholesterol does not affect NPC2 function. Purified NPC2 was delipidated through acetone precipitation. NPC2 was added at the indicated concentrations to *npc2* fibroblasts in lipid-free media with or without 1 μM cholesterol. After 3 days, cells were filipin stained and the fluorescence was quantified as described in *Materials and Methods*. The EC_{50} of the curve does not change significantly with or without cholesterol. (*B*) NPC2 can rescue individual transiently transfected *npc2* cells. *npc2* fibroblasts transiently transfected with NPC2-myc-his and GFP (10:1) to mark transfected cells were filipin-stained 3 days posttransfection. (*Left*) GFP fluorescence. (*Center*) Filipin fluorescence. (Bar = 20 μM.) Over 40% of GFP-positive cells were fully rescued (fluorescence in all pixels <750 units), and 23% were partially rescued (fluorescence between 750 and 1,000 units) when transfected with wild-type NPC2-myc-his. An anti-myc protein blot demonstrates that whereas D7A and I15F are expressed similarly to wild type, the amount secreted into the media is drastically reduced. Transfection of the mutants still resulted in a substantial fraction of fully (17 and 13%) and partially (27 and 31%) rescued cells, indicating that secretion is likely not required for rescue.

regardless of whether there is cholesterol in the medium (Fig. 5*A*). The dose–response curves for rescue by delipidated NPC2 are not significantly different with or without 1 μM cholesterol added to lipid-free media (EC_{50} = 1.6 nM vs. 1.1 nM; $P = 0.54$). Second, transient transfection of *NPC2* rescues individual transfected *npc2* cells while having no effect on adjacent cells (Fig. 5*B*), so secretion and cholesterol binding outside the cell do not seem to be necessary for rescue. Rescue occurs even when cells are transfected with NPC2 mutants that are very poorly secreted (Fig. 5*B*), so the protein appears to function without secretion or at least without release. Two mutated forms of the protein (D7A and I15F) are synthesized at levels similar to wild type but are secreted at <10% of the wild-type level. These mutant proteins are still able to rescue *npc2* cells that have been transiently transfected, although not as well as wild-type protein. We cannot completely rule out the possibility that the very small amount of secreted mutant NPC2 protein is responsible for the rescue.

Discussion

We have demonstrated the strength and specificity of the interaction between NPC2 and cholesterol. Our finding that the K_d is nearly two orders of magnitude lower than previously reported is important in establishing cholesterol binding as a real interaction that likely does occur *in vivo*. One source of the difference between our results and the lower-affinity binding reported by Okamura *et al.* (10) may come from carrying out the binding at 30°C instead of 0°C; in our experiments, full binding at 0°C was not achieved even after 1 h.

Amino Acids Required for Cholesterol Binding Form a Hydrophobic Binding Pocket. The three point mutants that have a reduced ability to bind cholesterol and rescue *npc2* cells provide new evidence that cholesterol binding is essential for the function of the NPC2 protein. The significance and meaning of these findings are clarified by the recent crystallization of the NPC2 protein (Friedland *et al.*, ref. 11). Mapping the three cholesterol-binding mutants (F66A, V96F, and Y100A) onto the structure shows that the three mutated residues are located in close proximity to each other in a hydrophobic region at one end of the β sandwich structure of the protein (Fig. 6*A*). The crystal structure reveals three small adjacent cavities just under these residues (Fig. 6*A*). The distance from the surface of the protein to the deepest of the three cavities is 18 Å, similar to the length of the cholesterol molecule. Although each of these cavities is smaller than cholesterol, it is possible that the two β-sheets shift or flex when the protein is in solution to create a single cavity wide enough to accommodate cholesterol. Indeed, the NMR structure of Der p 2 shows higher rms deviation in this part of the protein, possibly indicative of a high degree of mobility (24).

We propose that NPC2 binds cholesterol in this pocket, with the alkyl chain of cholesterol buried within the NPC2 protein and the hydroxyl group solvent exposed and possibly involved in a hydrogen bond with K97. F66 and Y100 may interact through ring stacking with cholesterol, whereas the V96F mutation may sterically block binding in the cavity. Loss of the proposed hydrogen bond does not appear to be sufficient to greatly disrupt NPC2 function, because K97A-conditioned media rescued 80% as well as wild type.

Four Functional Regions in NPC2. In our evolutionary analysis, we identified four regions (ECRs A, B, C, and D) that we predicted would be important for NPC2 function. Only one of these regions, ECR D in the vicinity of amino acid 101, appears to be primarily involved in cholesterol binding. Two of the mutations that reduced binding as well as rescue activity, V96F and Y100A, are located in this ECR. The third mutation that affects cholesterol binding, F85A, falls outside any of the ECRs but affects a single conserved residue.

The other three ECRs appear to have functions distinct from cholesterol binding. ECR A (centered around amino acid 9) contains the two amino acids identified as necessary for efficient secretion (D7 and I15). These two amino acids are in close proximity to each other in the NPC2 crystal structure (Fig. 6*B*). Although NPC2 mutated at either residue was able to rescue *npc2* fibroblasts by transient transfection, the secretion of NPC2 may have a more important function in specific tissues. The secreted protein may play a specialized role in organs such as the testes, where it may facilitate sperm maturation in the epididymal fluid (10).

Mutations in ECRs B and C (centered around amino acids 35 and 74, respectively) cause a reduction in NPC2 activity without affecting cholesterol binding. K32, in ECR B, is near the opening of the proposed binding pocket but positioned with its amino group pointing outward from the protein. D72 and K75 are in ECR C, on an entirely different surface of the protein (Fig. 6*B*). The charges of these residues and their surface locations suggest

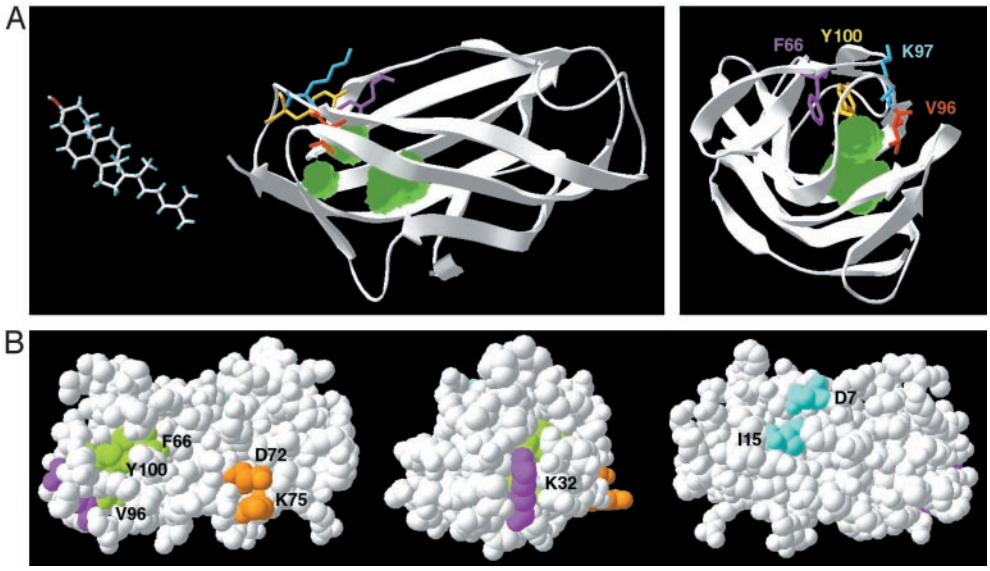

Fig. 6. Four functional regions of NPC2. (*A*) A proposed cholesterol-binding site. Two views of the NPC2 crystal structure (Friedland *et al.*, ref. 11) are shown in ribbons, with four key residues shown in stick representation. Three cavities detected within the crystal structure are shown in green. F66 (magenta) and Y100 (yellow) are proposed to be involved in ring-stacking interactions with cholesterol. The phenylalanine substitution at V96 (red) is proposed to project into the cavity (see especially *Right*) to sterically hinder cholesterol binding. (*B*) Assignment of functional regions on the NPC2 crystal structure. Three views of space-filling models of the NPC2 structure. Amino acids implicated in cholesterol binding (F66, V96, and Y100) are in green. D7 and I15 are required for efficient secretion of the protein and are in cyan. Two other regions of the protein marked in magenta (K32) and orange (D72 and K75) do not have a known function at this time. All of the residues are colored in the same hue as their corresponding ECR in Fig. 3, except for F66, which does not fall within an ECR.

interactions with other proteins that may work in concert with NPC2 to maintain normal cholesterol levels.

Why Does NPC2 Bind Cholesterol? NPC2 could bind cholesterol for any of several reasons: (*i*) Cholesterol binding by NPC2 could be required for sterol transfer between specific types of membrane. In this mode, NPC2 could bind cholesterol within the lumen of endosomes and control its transport from internal membranes to the limiting membrane that encloses the organelle. This type of function is analogous to the intermembrane transport of fatty acids carried out by members of the cytosolic lipid-binding protein family (reviewed in ref. 25). These proteins have a β sandwich fold like NPC2. (*ii*) Cholesterol binding could positively regulate some other event, such as an interaction between NPC2 and another protein that is required for maintaining normal cholesterol levels. A variation would be cholesterol-triggered activation of a catalytic function of NPC2. In this model, NPC2 would serve as a sensor of cholesterol concentration; the relevant cholesterol could be either inside or outside the cell. Our finding that varying extracellular cholesterol levels does not modulate NPC2 activity is evidence against the possibility that NPC2 is secreted to sense extracellular cholesterol levels. (*iii*) NPC2 could bind to cholesterol-rich membranes and, through protein–protein interactions, could influence the localization of other proteins, such as NPC1, that mobilize lipids. Such control of subcellular localization is exemplified by proteins with lipid-controlled signaling domains such as PKC, pleckstrin homology, or FYVE domains (reviewed in ref. 26). However, unlike NPC2, these proteins do not have a buried hydrophobic pocket and instead bind the lipid head group on their surfaces. On the basis of this structural consideration, localization to cholesterol-rich membranes is unlikely to be the purpose of NPC2 cholesterol binding. (*iv*) Cholesterol binding could negatively regulate an activity or event. Our mutants show that loss of cholesterol-binding activity results in a protein with reduced rescue activity, so this fourth possibility is unlikely.

Our evidence is consistent with cholesterol binding to NPC2 serving to transfer cholesterol between membranes and/or positively regulating an activity that maintains normal cholesterol levels. The most likely model incorporates both ideas: NPC2 may bind cholesterol from internal lysosomal membranes, which could positively regulate a physical interaction with NPC1 or another protein that directs the postlysosomal export of cholesterol through vesicular or nonvesicular means. In this way, NPC2 would act catalytically in moving cholesterol out of the lysosome, consistent with our finding that ≈3,000 cholesterol molecules are mobilized by each molecule of NPC2 in rescuing *npc2* fibroblasts. A similar mechanism is used by the GM2-activator protein, responsible for a subset of GM2 gangliosidoses cases (reviewed in ref. 27). This β sandwich protein (28) binds and solubilizes GM2 from internal lysosomal membranes and presents GM2 to β-hexosaminidase A for hydrolysis.

We thank Natasha Friedland, Ann Stock, and Peter Lobel for providing the NPC2 crystal structure and other useful information before publication and for critiques of the manuscript. We thank Eszter Vladar for help in obtaining the NPC2 point mutants, Karl Willert for help in the purification of NPC2, and Gregor Zimmermann for much useful discussion regarding the cholesterol-binding assay. We also thank Emily Ray for providing valuable advice and reagents. D.C.K. was supported by a Medical Scientist Training Grant. M.P.S. is an Investigator of the Howard Hughes Medical Institute. We are especially grateful to the Ara Parseghian Medical Research Foundation for support of this research.

1. Patterson, M. C., Vanier, M. T., Suzuki, K., Morris, J. A., Carstea, E. D., Neufeld, E., Blanchette-Mackie, E. J. & Pentchev, P. G. (2001) in *The Metabolic and Molecular Bases of Inherited Disease*, eds. Scriver, C. R., Beaudet, A. L., Sly, W. S. & Valle, D. (McGraw–Hill, New York), pp. 3611–3633.
2. Liscum, L. & Faust, J. R. (1987) *J. Biol. Chem.* **262,** 17002–17008.
3. Pentchev, P. G., Comly, M. E., Kruth, H. S., Tokoro, T., Butler, J., Sokol, J., Filling-Katz, M., Quirk, J. M., Marshall, D. C., Patel, S., *et al.* (1987) *FASEB J.* **1,** 40–45.
4. Kobayashi, T., Beuchat, M. H., Lindsay, M., Frias, S., Palmiter, R. D., Sakuraba, H., Parton, R. G. & Gruenberg, J. (1999) *Nat. Cell Biol.* **1,** 113–118.
5. Carstea, E. D., Morris, J. A., Coleman, K. G., Loftus, S. K., Zhang, D.,

Cummings, C., Gu, J., Rosenfeld, M. A., Pavan, W. J., Krizman, D. B., *et al.* (1997) *Science* **277,** 228–231.
6. Loftus, S. K., Morris, J. A., Carstea, E. D., Gu, J. Z., Cummings, C., Brown, A., Ellison, J., Ohno, K., Rosenfeld, M. A., Tagle, D. A., *et al.* (1997) *Science* **277,** 232–235.
7. Naureckiene, S., Sleat, D. E., Lackland, H., Fensom, A., Vanier, M. T., Wattiaux, R., Jadot, M. & Lobel, P. (2000) *Science* **290,** 2298–2301.
8. Millat, G., Chikh, K., Naureckiene, S., Sleat, D. E., Fensom, A. H., Higaki, K., Elleder, M., Lobel, P. & Vanier, M. T. (2001) *Am. J. Hum. Genet.* **69,** 1013–1021.
9. Kirchhoff, C., Osterhoff, C., Habben, I., Ivell, R. & Kirchloff, C. (1990) *Int. J. Androl.* **13,** 155–167.
10. Okamura, N., Kiuchi, S., Tamba, M., Kashima, T., Hiramoto, S., Baba, T., Dacheux, F., Dacheux, J. L., Sugita, Y. & Jin, Y. Z. (1999) *Biochim. Biophys. Acta* **1438,** 377–387.
11. Friedland, N., Liou, H.-L., Lobel, P. & Stock, A. M. (2003) *Proc. Natl. Acad. Sci. USA* **100,** 2512–2517.
12. Cadigan, K. M., Spillane, D. M. & Chang, T. Y. (1990) *J. Cell Biol.* **110,** 295–308.
13. Simon, A. L., Stone, E. A. & Sidow, A. (2002) *Proc. Natl. Acad. Sci. USA* **99,** 2912–2917.
14. Thompson, J. D., Higgins, D. G. & Gibson, T. J. (1994) *Nucleic Acids Res.* **22,** 4673–4680.
15. Friedman, N., Ninio, M., Pe'er, I. & Pupko, T. (2002) *J. Comput. Biol.* **9,** 331–353.
16. Kelley, L. A., MacCallum, R. M. & Sternberg, M. J. (2000) *J. Mol. Biol.* **299,** 499–520.
17. Fischer, D., Barret, C., Bryson, K., Elofsson, A., Godzik, A., Jones, D., Karplus, K. J., Kelley, L. A., MacCallum, R. M., Pawowski, K., *et al.* (1999) *Proteins* Suppl. 3, 209–217.
18. Guex, N. & Peitsch, M. C. (1997) *Electrophoresis* **18,** 2714–2723.
19. Lange, Y., Swaisgood, M. H., Ramos, B. V. & Steck, T. L. (1989) *J. Biol. Chem.* **264,** 3786–3793.
20. Lange, Y., Ye, J. & Steck, T. L. (1998) *J. Biol. Chem.* **273,** 18915–18922.
21. Davies, J. P., Chen, F. W. & Ioannou, Y. A. (2000) *Science* **290,** 2295–2298.
22. Rossjohn, J., Feil, S. C., McKinstry, W. J., Tweten, R. K. & Parker, M. W. (1997) *Cell* **89,** 685–692.
23. Tsujishita, Y. & Hurley, J. H. (2000) *Nat. Struct. Biol.* **7,** 408–414.
24. Mueller, G. A., Benjamin, D. C. & Rule, G. S. (1998) *Biochemistry* **37,** 12707–12714.
25. Storch, J. & Thumser, A. E. (2000) *Biochim. Biophys. Acta* **1486,** 28–44.
26. Hurley, J. H. & Misra, S. (2000) *Annu. Rev. Biophys. Biomol. Struct.* **29,** 49–79.
27. Mahuran, D. J. (1998) *Biochim. Biophys. Acta* **1393,** 1–18.
28. Wright, C. S., Li, S. C. & Rastinejad, F. (2000) *J. Mol. Biol.* **304,** 411–422.